Raman Spectra and Structural Data of the Nanocrystalline KTP (KTiOPO$_4$) Synthesized by Pechini Method

R. Malekfar[a,*], A. Cheraghi[a,b], G. Ahmadi[c] and M. Khanzadeh[c]

[a]Physics Department, Faculty of Basic Sciences, Tarbiat Modares University

P.O. Box 14115-175, Tehran, I.R. Iran

[b]Faculty of Sciences, Shahid Sattari University, Tehran, I.R. Iran

[c]Physics Department, Valieasr University of Rafsanjan, Rafsanjan, I.R. Iran

Nanocrystalline KTP powders are synthesized using a modified Pechini method. The structural and lattice modes of the products are investigated via X-ray diffraction, micro Raman backscattering spectroscopy, UV/vis/NIR and FT-IR transmission spectroscopy. The Debye–Scherrer formula is used to confirm the grain sizes estimated by the scanning electron microscopy slides.

PACS numbers: 78.30.−j, 77.84.Fa

1. Introduction

Potassium titanyl phosphate (KTiOPO$_4$, KTP) was first introduced as a nonlinear optical material in 1976 [1]. Its high thermal stability, good mechanical characteristics, optical transparency over a large wavelength range, large nonlinear coefficients, high damaged threshold and broad angular acceptance have made it the standard material in industrial and medical applications [2, 3]. It is also an important building block in laser systems using frequency conversion, such as the second harmonic generation (SHG) and optical parametric oscillators (OPOs) [4].

In recent years nanostructured materials have been intensively studied by many scientists. The sol-gel technique has been widely used as an alternative method for preparing glass, moonlights, fibers, nanostructured powders and thin films or coatings of inorganic materials. In comparison to the traditional techniques, sol-gel method has many advantages such as control over purity and composition, easy introduction of doping elements, preparation of hybrid materials, and low temperature processing [5].

The Pechini method [6] has been used as an alternative to the conventional sol-gel technique because of low cost, versatility, control of the stoichiometry, its simplicity, low processing temperature, high degree of homogeneity due to the fact that reagents are mixed at the molecular level [7]. The product can be easily used to synthesize other more advanced materials, such as nanocomposites [8, 9].

In our method, first the chelates are formed between metal ions and an a-hydroxycarboxylic acid (citric acid, CA). In the next step, a polyhydroxyl alcohol (ethylene glycol, EG) is added and heated to obtain polymeric resin. Heating process on the polymeric resin at 573 K causes a breakdown of the polymer. Final step is the calcinations process for several hours to breakdown polymer at known temperature to obtain the nanocrystalline material [7].

In this study a modified Pechini method, we believe for the first time, is used to synthesize nanocrystalline KTP. Consequently the products are characterized by X-ray diffraction (XRD), near normal reflection FT-IR spectroscopy, UV/vis/NIR spectroscopy and micro-Raman backscattering.

2. Experimental procedure

K$_2$CO$_3$ (Merck 99.5%), TiO$_2$ (Merck 99.5%), ethylenediaminetetraacetic acid (EDTA) (Merck 99.5%), EG (Merck pure), (NH$_4$)$_2$HPO$_4$ (Merck 99.5%) is used as raw material. Because of strong chelating power of EDTA, we used it for chelating metallic ions.

The precursor solution of Ti, K, and P is prepared by adding raw materials into an aqueous solution of EDTA and EG heating and stirring. By increasing the temperature of solution to 373 K in a steady stage and within 1–2 h, the solution changes to resin with high viscosity. A further calcination process at 575 K for 2 h breaks the resin; consequently, another calcination process is carried at 973 K for several hours. The molar ratio of metallic ions, EDTA and EG is a very important factor for an optimum grain sizes of the products and in this work we adapted the ratio as 1:2:6.

* corresponding author; e-mail: `Malekfar@Modares.ac.ir`

3. Results and discussions

3.1. Raman spectra analysis

The Raman spectra of the grown nanocrystallites of KTP were collected at the Spectroscopy Laboratory, Atomic and Molecular Group, Physics Department, Tarbiat Modares University by using a Thermo Nicolet Almega dispersive micro-Raman scattering spectrometer operating by a 532 nm laser line as the second harmonic of a Nd:YLF laser.

A very typical of the recorded micro Raman backscattering spectra has been presented in Fig. 1. The analysis of the Raman active modes of the samples can be carried out according to the standard symmetrical analysis and selection rules correlation of the normal modes.
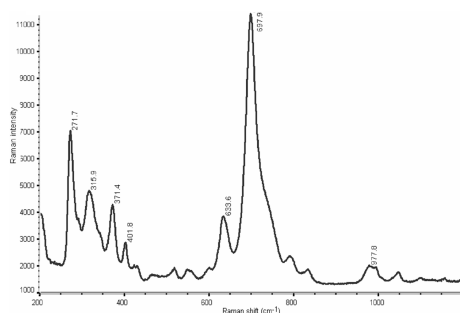

Fig. 1. A typical recorded Raman spectrum of the synthesized KTP nanocrystallites calcinated at $650\,°C$ for 8 h, in the spectral region of $200–1300\ cm^{-1}$.

In the lattice the TiO_6 octahedral and PO_4 tetrahedral units exist. The normal vibrations of each of these units can be carried out and we can summarize the results as the followings:

(I) Three modes with very strong, strong, and medium intensities at 697.9, 271.7 and $201.2\ cm^{-1}$ have been assigned to ν_1 symmetric, ν_5 and ν_6 modes of TiO_6, respectively. Two modes with medium intensities at 633.6 and $315.9\ cm^{-1}$ have been assigned to ν_2 and ν_4 modes of TiO_6 unit, respectively [10].

(II) For the PO_4 unit, four Raman active modes at 977.8, 422.6, 1045.9, and $547.8\ cm^{-1}$ have been assigned to ν_1, ν_2, ν_3 and ν_4 modes of the unit, respectively.

(III) There are also some weak and medium intensities bands in the low wave numbers of the Raman spectra. They are due to the external modes of the lattice vibrations. Few weak bands are present in the higher frequency part of the ν_3 Raman active mode of PO_4, at $1045.9\ cm^{-1}$. They have central part wave numbers of 1097.8 and $1166.8\ cm^{-1}$. They can be assigned to the combination bands of the internal and external lattice modes. Figure 1 shows a typical recorded micro Raman backscattering spectrum of the grown KTP nanocrystallite in the external, internal, and combination bands of the PO_4 and TiO_6 units [11, 12].

In overall conclusion, the recorded Raman spectra are in close consistency with the previously recorded Raman spectra for the single crystal of KTP by Bushiri et al. investigation [13]. There are some shifts in the lower parts of the spectra due to the quantum confinement of the nanoparticles of the samples.

3.2. FT-IR transmission spectroscopy

The FT-IR spectra of the grown samples were collected by using a Thermo Nicolet Nexus 760 FT-IR spectrometer system. The recorded FT-IR bands of the synthesized KTP nanocrystallites can be described as follows.

The bands corresponding to the ν_{as} and ν_s vibrations of P–O: All bands at the higher wave numbers are rather wide and their number is smaller due to the increase of lattice symmetry $(4/m)$ in comparison with $KTiOPO_4$ $(mm2)$. The vibration band corresponding to Ti–O fragment has been assigned at $706.1\ cm^{-1}$ in $KTiOPO_4$ (Fig. 2). It clearly shows that six resolved bands at 973.9, 995, 1025.2, 1048.7, 1101.2, and $1124.8\ cm^{-1}$, are associated with the asymmetric ν_2 stretching vibration (the ν_2 vibration is threefold degenerate) of PO_4 units.
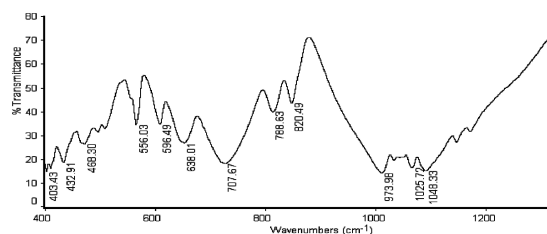

Fig. 2. FT-IR transmission spectrum of the synthesized KTP nanocrystallites.

3.3. XRD analysis

The X-ray diffraction patterns of the samples are collected by an Xpert X-ray diffractometer model 1480 manufactured by Philips.

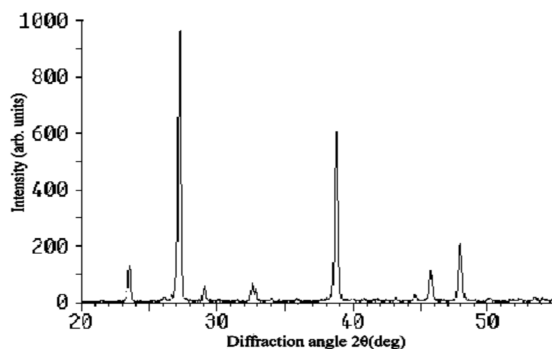The XRD patterns of the nanocrystal KTP heat-treated at $850\,°C$ are shown in Fig. 3.

Fig. 3. X-ray powder diffraction pattern of typical synthesized KTP nanocrystallites.

It is clear from Fig. 3 that the crystalline phase is present in the sample. All peaks in XRD patterns are

assigned to KTP and eight intense peaks were detected at 23°, 27°, 29°, 32°, 32.8°, 34°, 38°, 45°, and 50°. These peaks are indexed to the diffraction lines from (101), (311), (013), (301), (411), (004), (015), (501), and (603), respectively. The agreement between the XRD and the standard data in JCPDS file confirms the precipitation of KTP. However, relative intensities of some major peaks such as (212) and (402) are inconsistent with KTP standard data. It should also be noted that there are some signs of some residual amorphous phase in the XRD pattern [5].

3.4. Scanning electronic microscope imaging

A scanning electron microscopy (SEM) study of the produced samples showed that the grains of crystalline powders formed were almost round-shaped (Fig. 4). The nanocrystalline sizes were determined to be in the range of 50–100 nm. However, the sizes of grains also were calculated by the Debye–Scherrer relation using the XRD patterns and they were found to be in the range of 80–90 nm which is in close agreement with the SEM imaging results. It was found that the size and the number of the grains of the nanocrystalline powders were increased by increasing the calcination temperature.
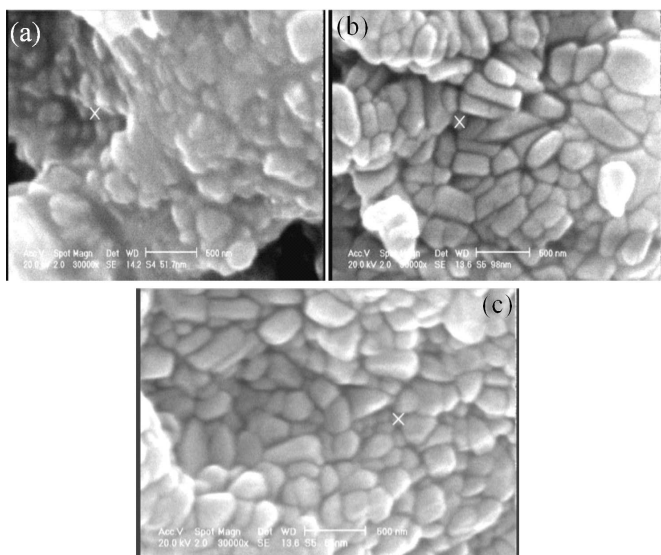

Fig. 4. SEM imaging of synthesized KTP nanocrystallites at different calcination temperature: (a) 700 °C, 8 h; (b, c) 750 °C, 10 h.

3.5. UV-vis-NIR spectroscopy

The transmission spectra of KTP were measured using a PG Instrument UV-Visible Spectroscope, model T80+. We used the solution of KTP in ethanol. The cut-off wavelength was measured to be about 340 nm (Fig. 5) which is almost in agreement with other investigations in the present study [14].
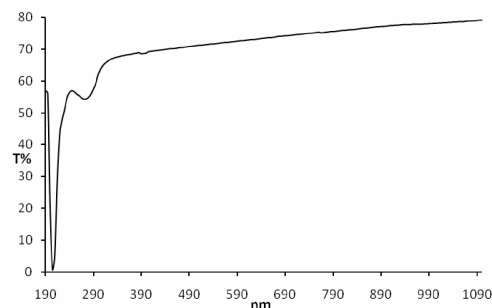

Fig. 5. UV/vis/NIR transmission spectrum of the synthesized KTP nanocrystallites.

4. Conclusions

Nanocrystalline KTP with the SEM estimation of the grain size of 50–100 nm is synthesized by modified Pechini method. EDTA is employed as a chelating agent in production of the nanoparticles. The Debye–Scherrer grain size calculation using the X-ray diffraction patterns agrees with the SEM results. Micro-Raman scattering, FT-IR transmission and UV/vis/NIR spectroscopies were used to assign the relevant recorded active modes encountered.

References

[1] F.C. Zumsteg, J.D. Bierlein, T.E. Gier, *J. Appl. Phys.* **476**, 4980 (1976).

[2] J.D. Bierlein, A. Ferretti, L.H. Brizner, W.Y. Hsu, *Appl. Phys. Lett.* **50**, 1216 (1987).

[3] J.D. Bierlein, H. Vanherzeele, *J. Opt. Soc. Am. B* **6**, 622 (1989).

[4] I. Koseva, V. Nikolov, P. Peshev, *J. Alloys Comp.* **353**, L1 (2003).

[5] D. Li, L. Kong, L. Zhan, X. Yao, *J. Non-Cryst. Solids* **271**, 45 (2003).

[6] M.P. Pechini, *U.S. Patent* No. 3.33, 1967, p. 679.

[7] J.J. Carrajal, M. Galceran, M.C. Pujol, F. Diaz, M. Aguilo, in: *15th Int. Conf. on Crystal Growth, Utah (USA) 2007.*

[8] M. Galceran, M.C. Pujol, J.J. Carvajal, S. Tkaczyk, I.V. Kityk, F. Díaz, M. Aguiló, *Nanotechnology* **20**, 035705 (2009).

[9] S. Tkaczyk, M. Galceran, S. Kret, M.C. Pujol, M. Aguiló, F. Díaz, A.H. Reshak, I.V. Kityk, *Acta Mater.* **56**, 5677 (2008).

[10] A.A. Babaryk, I.V. Zatovsky, V.N. Baumer, N.S. Slobodyanik, P.G. Nagorny, O.V. Shishkin, *J. Solid State Chem.* **180**, 1990 (2007).

[11] J.C. Jacco, *Mater. Res. Bull.* **21**, 1189 (1986).

[12] L.W. Daasch, D.C. Smith, *Anal. Chem.* **23**, 853 (1951).

[13] M.J. Bushiri, V.P. Mahadevan Pillai, R. Ratheesh, V.U. Nayar, *J. Phys. Chem. Solids* **60**, 1983 (1999).

[14] S. Ganesa Moorthy, F. Joseph Kumar, S. Balakumar, C. Subramanian, *J. Mater. Sci. Eng. B* **60**, 88 (1999).